Journal of Electromyography and Kinesiology 45 (2019) 18–25

Contents lists available at ScienceDirect

Journal of Electromyography and Kinesiology

journal homepage: www.elsevier.com/locate/jelekin

Single-trial estimation of quasi-static EMG-to-joint-mechanical-impedance relationship over a range of joint torques

Chenyun Dai[a], Stephane Martel[c], Francois Martel[d], Denis Rancourt[d], Edward A. Clancy[b,*]

[a] Department of Electrical Engineering, Fudan University, Shanghai, China
[b] Department of Electrical and Computer Engineering, Worcester Polytechnic Institute, Worcester, MA 01609, USA
[c] BRP US Management, Inc., El Paso, TX 79935, USA
[d] Groupe de Recherche Perseus, Département de Génie Mécanique, Faculté de Génie, Université de Sherbrooke, Sherbrooke, QC J1K 2R1, Canada

ARTICLE INFO

Keywords:
Physiologic modeling
Electromyography
Least squares estimation
Joint impedance

ABSTRACT

Joint mechanical impedance is commonly measured by applying dynamic perturbations about a joint at a fixed operating point/background torque, and quantifying torque change vs. angle change. Impedance characterization in functional tasks, therefore, requires multiple experimental trials over a range of operating points—a cumbersome, invasive, time-consuming and impractical task. As an alternative, studies have related EMG to impedance, after which EMG can estimate impedance without applying joint perturbations. But, the cumbersome calibration trials are still required. We describe a method of single contraction perturbations in which the background torque slowly ramps over the operating range, with EMG simultaneously acquired. Using one such "quasi-static" contraction for model training and another for testing, we show this method to be a reasonable surrogate for traditional second-order, linear impedance modeling. A simple, short-duration calibration results. We compared our single-trial ramp method to multiple constant background torque trials at 10, 20, 30, and 40% maximum effort (extension and flexion), finding only limited differences in traditional vs. EMG-based ramp impedance estimates (12–22%, most prominent at the two lower contraction levels). Such constant force and slowly-variable force contractions are relevant to many practical applications, including ergonomics assessment, prosthetic control and clinical biomechanics.

1. Introduction

A plethora of studies relate the surface electromyogram (EMG) to joint torque, as a means of non-invasively estimating musculoskeletal loads and joint/musculoskeletal dynamics (An et al., 1983; Clancy et al., 2006, 2012; Clancy and Hogan, 1997; Doheny et al., 2008; Gottlieb and Agarwal, 1971; Hashemi et al., 2013, 2015, 2012; Liu et al., 2015; Staudenmann et al., 2010; Thelen et al., 1994; Vredenbregt and Rau, 1973). Measurement and understanding of these dynamics is important in several applied areas, including: ergonomic assessment (Hagg et al., 2004), prosthetic control (Parker et al., 2006), and clinical biomechanics (Disselhorst-Klug et al., 2009; Doorenbosch and Harlaar, 2003). A distinct aspect of musculoskeletal loading, but of equal importance, is the joint mechanical impedance (characterized by stiffness, viscosity, and inertia parameters—assuming a linear model). A joint usually exhibits non-zero mechanical impedance as it produces a reaction torque when it is subjected to a generalized displacement. Joint impedance is a necessary property of the musculoskeletal system because it helps stabilize force interactive tasks such as tool usage (Burdet et al., 2001; Tee et al., 2010). Joint mechanical impedance can be modulated independently of joint torque by co-contracting agonist-antagonist muscles about the joint. For example, a worker using a power tool (e.g., a hand drill) will purposely co-contract their muscles to increase hand mechanical impedance up to *at least* the minimum required to stabilize the task (Rancourt and Hogan, 2001a, b), while providing the required hand force on the tool. Impedance formally characterizes the torque-angle relationship state of the joint, and does so using an absolute physical scale (e.g., the stiffness component of linear impedance models is expressed in units of Newton-meters per radian) as opposed to the non-dimensional measures that are common based on EMG activation levels (Andison, 2011; Ford et al., 2008; Rosa et al., 2014). Accurate measurement of joint mechanical impedance in daily activities may provide new insights into the origin of several musculoskeletal disorders.

Impedance has been measured in numerous settings, including: during constant-posture tasks at a constant background torque level/

* Corresponding author at: Worcester Polytechnic Institute, Department of Electrical and Computer Engineering, 100 Institute Road, Worcester, MA, United States.
E-mail address: ted@wpi.edu (E.A. Clancy).

https://doi.org/10.1016/j.jelekin.2019.02.001
Received 4 October 2018; Received in revised form 4 February 2019; Accepted 5 February 2019

operating point (see below), point-to-point motion tasks (Burdet et al., 2001), with forces applied to the hand from different directions (Gomi and Osu, 1998; McIntyre et al., 1996), and during various dynamic movements (Bennett et al., 1992; Ludvig et al., 2017; MacNeil et al., 1992; Rouse et al., 2014). Studies have separated stiffness due to the intrinsic properties of the muscle and joint from stiffness due to stretch reflex feedback (Golkar et al., 2017; Guarin and Kearney, 2018; Kearney et al., 1997; Zhao et al., 2008). Separating stiffness components is useful for understanding the physiology and motor control aspects of human actuation and movement. For applied studies (the interest of this research), however, it is the total impedance that is of interest. Our experimental work described herein focused on total impedance.

Concentrating on constant-posture tasks at a static/quasi-static background torque level (the conditions associated with this experimental report), mechanical impedance has been estimated by imparting forces (inputs) on the body with a manipulandum and measuring the resulting change in position/angle (outputs), or vice versa (Bennett et al.,1992; Burdet et al., 2001; Cannon and Zahalak, 1982; Gomi and Osu, 1998; Hunter and Kearney, 1982; Kearney and Hunter, 1990; Kearney et al. 1997; McIntyre et al., 1996; Zhang and Rymer, 1997). Methods of system identification are then used to build dynamical mathematical models that relate the system inputs to their outputs. Classical impedance modeling methods have performed well for their intended scientific studies, but have some important limitations for broader applications. Firstly, numerous measurement trials (minimum of one per operating point) have been required to characterize impedance over a range of operating conditions. For example, if perturbations are imparted about a nominal joint angle at a nominal torque level, then the impedance relationship is well characterized via the *stiffness, viscosity, and inertia* of a second-order linear system (Kearney and Hunter, 1990; Zhang and Rymer, 1997). Perturbation trials conducted at distinct background torque levels are needed to separately characterize the system at each torque level (a.k.a. operating point). Secondly, such measurements require imparting forces on the body segments, disturbing the task under study, a situation quite undesirable for taking in situ measurements during field tasks.

Recent studies have characterized impedance over a range of operating points (Golkar et al., 2017; Ludvig and Perreault, 2012). These studies have separated intrinsic stiffness from reflex stiffness—an important goal for scientific studies—but, in doing so, have necessarily included advanced nonlinear model structures with concomitantly complex solution methods. Models have included parallel-cascade forms with Hammerstein nonlinear systems (Guarin and Kearney, 2018), as well as a "Skirt Decomposition" technique in which the input perturbation is a multisine (i.e., comprised of the sum of a small number of sine waves, with the assumption of smooth behavior between the evaluated frequency locations) (Cavallo et al., 2018; de Vlugt et al., 2003). These model forms can provide a wealth of useful scientific information, but their complexity make them unlikely to be routinely adopted in applied studies, particularly when only the total impedance is desired to be measured. In other words, when intrinsic and reflex stiffness need not be separated in applied studies, the complex signal processing methods are not as attractive.

Considering existing technologies, surface electromyography (EMG) may be an excellent solution to simultaneously estimate torque and impedance during applied motor tasks as it provides a non-invasive approach (after calibration with a manipulandum). Previous work has successfully related EMG to joint *quasi-stiffness*—which does not seek to account for short-range stiffness (Rack and Westbury, 1974; Rouse et al., 2013). Osu and Gomi (1999) assumed a baseline stiffness representing passive joint properties and a second additive quasi-stiffness component proportional to muscular activity of both agonist and antagonist muscles of the joint. Others have successfully related EMG to joint quasi-stiffness in various tasks by differentiating the EMG-torque relationship as a function of joint angle (Kawase et al., 2012; Pfeifer et al., 2012; Shin et al., 2009). These methods are attractive in that only simpler torque measurements are required in order to calibrate the model. But, the model identification process utilizes multiple trials which are cumbersome for applied studies, the model form is limited by the EMG-torque model, and no viscosity term is estimated. Of course, the inertial properties of human joints do not vary noticeably with the level of joint torque.

Our work described herein seeks to advance the established linear, second-order system estimates of total joint viscosity and stiffness (i.e., not separated into its intrinsic and reflex components) which use the standard method of mechanical perturbations at a fixed background torque level either as a direct estimate of joint impedance ("fixed-mechanical" model) or as a means to calibrate an EMG-impedance model ("fixed-EMG" model). First, we introduce methods in which the operating point ("background" torque level) is slowly ramped, such that a single perturbation trial is used to calibrate an EMG-impedance model over a continuous range of operating points/torques ("ramp-EMG" model). Second, we investigate the extent to which the single-trial ramp data, in the *absence* of EMG, can be used to model joint viscosity and stiffness ("ramp-mechanical" model). We used least-squares estimation to fit our models, as this technique is widely available, robust and, therefore, well suited for applied research. Our experimental evaluation was completed on human subjects producing torques about their elbow joint.

2. Methods

2.1. Experimental methods

The experimental work was approved by the Institutional Review Board (IRB) of Laval University (Québec, Canada) and the Worcester Polytechnic Institute IRB. All subjects provided written informed consent. Seven subjects (3 females, 4 males; aged 21–43 years) each participated in one experimental session. The skin above the investigated muscles was cleaned with alcohol and four bipolar EMG electrode-amplifiers placed transversely across each of the biceps and triceps muscles, midway between the elbow and the midpoint of the upper arm, centered on the muscle midline. The two contacts (5 mm diameter, stainless steel, separated 10 mm edge-to-edge) of each electrode-amplifier were oriented along the muscle's long axis. Adjacent electrodes were spaced ~1.75 cm apart. A reference electrode was applied over the acromion process. Each electrode-amplifier had a common mode rejection ratio greater than 90 dB at 60 Hz. EMG signals were highpass filtered at 15 Hz (eighth-order Butterworth) and then lowpass filtered at 1800 Hz (fourth-order Butterworth). A subject was seated in front of a planar joystick manipulandum (Fig. 1) that could produce 15 N m of torque (about 50 N at the tip) with a frequency response up to 15 Hz. The joystick actuated horizontal (medial-lateral) motion only, to elicit elbow flexion-extension. Subject's held their right arm in the plane parallel to the floor, with the shoulder abducted 90°, the forearm oriented in the sagittal plane, the wrist fully supinated and the elbow flexed 90°. A rigid cuff, extending from the distal forearm through the hand, was secured tightly to the subject and the manipulandum load cell, preventing wrist motion. The manipulandum allowed the cuff to slide freely along the direction of the long axis of the forearm to eliminate any undesired coupled stiffness that would result from the connection of the forearm to the joystick. The EMG signals were sampled at 4096 Hz and the load cell signal at 400 Hz (time synchronized), each using 16 bits.

Subjects initially performed two, 2 s maximum voluntary contractions (MVCs) in each of flexion and extension, the maximum of which was used as the subject's MVC. Next, they performed a 0% MVC (rest contraction) and separate flexion and extension 50% MVCs for 5 s, utilizing force feedback on a computer screen. These contractions were used to calibrate an advanced, four-channel, whitened EMG processor (detailed below) (Clancy and Farry, 2000; Prakash et al., 2005), which

Fig. 1. Top figure shows rear view of subject seated in the impedance measurement apparatus. Inset figure at lower left shows top view. Inset figure at lower right shows close-up view of subject's right hand-wrist rigidly cuffed to the actuated joy stick and load cell. Force perturbations were applied in the medial-lateral direction, to elicit elbow flexion-extension.

has been shown to exhibit lower variance (Clancy and Hogan, 1994, 1995; Hogan and Mann, 1980) and lower EMG-torque error (Clancy and Hogan, 1997; Clancy et al., 2012; Potvin and Brown, 2004). This advanced processor would be expected to produce EMG-impedance estimates that would also exhibit lower variance. Pseudo-random perturbations (manipulandum set in angle control, 0–6 Hz frequency range, Gaussian distributed with zero mean and std. dev. of 4°) were then performed twice for 20 s with the subject's arm secured in the cuff while the subject rested (0% MVC), to measure the baseline inertia (I_o), viscosity (B_o), and stiffness (K_o) of the combined arm-manipulandum system at rest. This narrower frequency range, as compared to the 0–15 Hz frequency range used thereafter for the active-contraction trials (see next paragraph), was required to keep the manipulandum stable, as it exhibited low viscosity and stiffness.

Subjects then performed two repetitions of eight distinct, 30 s duration, *fixed-background* perturbation trials (16 trials total, randomized in order). During a trial, the manipulandum exerted a constant background torque for 5 s, the same constant torque with superimposed torque perturbations for the next 20 s (0–15 Hz bandwidth pseudo-random, Gaussian distributed with zero mean and std. dev. of 0.8 N m), then returned to applying the same constant torque for the last 5 s (Fig. 2). Based on the previous measurements of MVC, the trials (randomly) cycled through one of eight constant torque levels corresponding to the subject-generated torque at 10%, 20%, 30%, or 40% MVC extension or flexion. During each trial, the orientation of the manipulandum was fed back to the subject on a computer screen. The subject was instructed to maintain their average elbow joint angle at 90° throughout the trial, countering the average torque applied by the manipulandum. Only the middle 20 s of data were used for analysis. The subject's forearm was removed from the wrist cuff between all trials for 2–3 min of rest to avoid fatigue.

A second set of *ramp* trials was conducted in which subjects

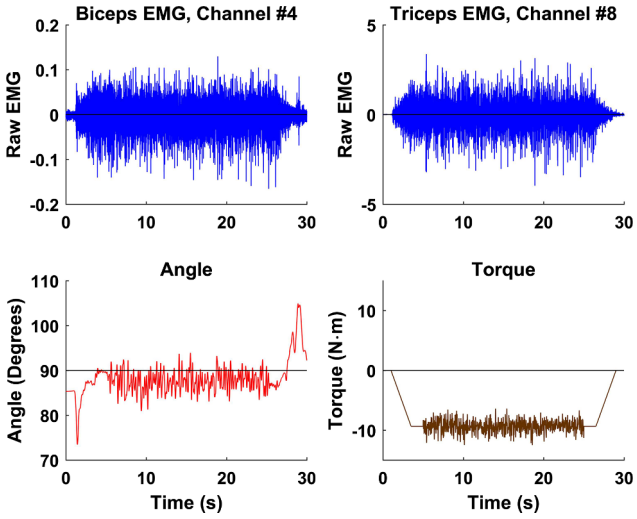

Fig. 2. Sample time-series data from a constant-torque ("fixed") trial, showing sample biceps EMG, triceps EMG, angle, and torque. (Subject 18, 40% extension trial 1.)

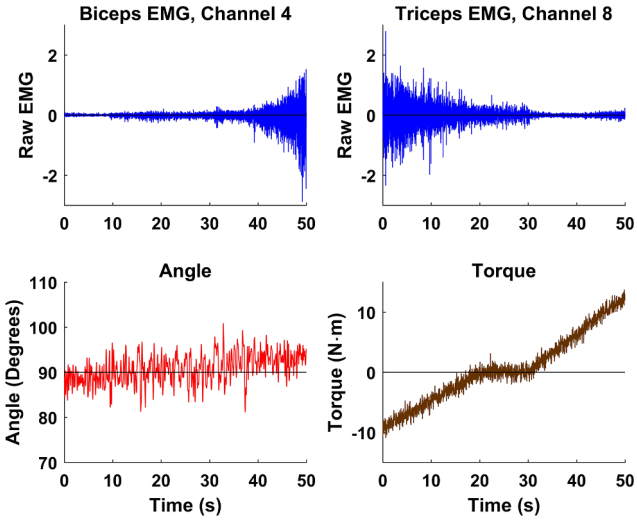

Fig. 3. Sample time-series data from a ramp torque trial, showing sample biceps EMG, triceps EMG, angle, and torque. (Subject 18, ramp trial 1.)

maintained their elbow joint angle at 90° while a ramp force, combined with continuous force perturbations, was exerted by the manipulandum over 50 s (Fig. 3). Each trial was segmented as: during the first 20 s, the nominal torque started at 40% MVC extension and linearly ramped to 0% MVC; during the next 10 s, the nominal torque was 0% MVC; and during the last 20 s, the nominal torque linearly ramped from 0% MVC to 40% MVC flexion. Three such trials were performed. The pause at 0% MVC was added after initial evaluation found it difficult for subjects to follow the nominal torque trajectory across zero.

2.2. Signal preprocessing

Analysis was performed offline in MATLAB. (See Supplementary Material, Fig. S1 for a graphical summary of the signal analysis steps.) All filter specifications reported herein refer to the designed filters—these filters were applied in the forward, then reverse, time directions to achieve zero phase (and the square of the designed magnitude response). Raw EMG signals were highpass filtered (15 Hz cutoff, 5th-order Butterworth). Then, two distinct EMG standard deviation (EMGσ) estimates were computed for each of extension and flexion—a single-channel, unwhitened estimate (using a centrally-located

electrode) and a four-channel, whitened estimate using adaptive whitening (Clancy and Farry, 2000; Prakash et al., 2005). Results using each of these EMG processors are separately presented below. Each used a first-order demodulator (rectifier), followed by lowpass filtering at 40 Hz (Chebyshev Type 1 filter, 9th-order, 0.05 dB peak-to-peak passband ripple) and then downsampling to 100 Hz. This lower rate is appropriate for system identification (Clancy et al., 2006; Ljung, 1999).

The general second-order linear mechanical joint impedance model at a particular operating point is (Kearney and Hunter, 1990):

$$\Delta T[m] = I\ddot{\theta}[m] + B\dot{\theta}[m] + K\Delta\theta[m] \quad (1)$$

where m is the resampled index, ΔT is the change in joint torque, $\Delta\theta$ is the change in joint angle; and I (inertia), B (viscosity) and K (stiffness) are the fit parameters. Since torque and angle *change* are required in Eq. (1), each of these corresponding measured signals (T and θ) was highpass filtered at 0.3 Hz using a 2nd-order Butterworth filter, to remove the "background torque trend." This approach was applicable to both constant-torque and ramp-torque trials. After highpass filtering, torque and angle were lowpass filtered at 40 Hz (same filter as the EMG signals) and then downsampled to 100 Hz to form $\Delta T[m]$ and $\Delta\theta[m]$. For the first derivative of angle, a central difference was computed, followed by 5th-order lowpass filtering with a Butterworth filter with cutoff frequency at 15 Hz. For the second derivative of angle, two successive central differences were computed, followed by the same lowpass filter. These filter selections were determined via preliminary analysis, and were critical in producing derivative estimates that attenuated high-frequency noise (Giakas and Baltzopoulos, 1997; Winter, 2005). These derivative estimates were downsampled to 100 Hz to form $\dot{\theta}[m]$ and $\ddot{\theta}[m]$.

2.3. System identification and statistics

For each subject, the two, 20 s duration, 0% MVC trials were combined and used to estimate the impedance parameters (inertia I_o, viscosity B_o, stiffness K_o) of the arm-manipulandum system at rest (Eq. (1)), using least squares. All least squares used the regularized pseudo-inverse technique in which singular values of the design matrix were removed if their ratio to that of the largest singular value was less than a tolerance value. Through preliminary analysis, a tolerance value of 0.005 was selected, similar to that used in EMG-force modeling (Clancy et al., 2012). In all subsequent analysis, the torque estimated via these 0% MVC trial parameters ($\Delta T_o[m]$) was subtracted from the overall torque, leaving only the torque change due to muscle activation. This step accounted for the dynamics of the manipulandum, since they interact with those of the arm (de Vlugt et al., 2003). In addition, the inertia I_o was set to the value computed at 0% MVC and not further estimated, as it does not noticeably change with muscular activation level.

Next, "fixed-mechanical" model viscosity and stiffness parameters were least squares estimated from joint torque and angle (Eq. (1)) of each constant-torque trial, *without* the use of EMG. The middle 20 s of data, avoiding the recording portions that did not include perturbations, were used. Parameter values were estimated separately for the eight contraction levels and two sets, with the results from the two trials per condition averaged. These parameter values served as the "true" parameter values, in that they were estimated via the established method.

Then, EMG signals were used to estimate "fixed-EMG" model viscosity and stiffness parameters from the constant-torque trials. EMGσ was incorporated into the joint mechanical impedance model of Eq. (1) in a linear fashion by setting:

$$B[m] = B_e\, EMG\sigma_e[m] + B_f\, EMG\sigma_f[m] \quad \text{and}$$
$$K[m] = K_e\, EMG\sigma_e[m] + K_f\, EMG\sigma_f[m] \quad (2)$$

giving the model:

$$\Delta T[m] = I_o\ddot{\theta}[m] + \{B_e EMG\sigma_e[m] + B_f EMG\sigma_f[m]\}\dot{\theta}[m] + \{K_e EMG\sigma_e[m] + K_f EMG\sigma_f[m]\}\Delta\theta[m] \quad (3)$$

where $EMG\sigma_e$ and $EMG\sigma_f$ are the EMGσ values for extension and flexion, respectively; and the B_i and K_i are the fixed-EMG viscosity and stiffness fit parameters, respectively. Again, the middle 20 s data segment was used for identification. A full set of eight trials (one per contraction level) was combined as training data, so that EMG would be related to impedance parameters across the range of effort levels. Formally, Eq. (3) is no longer linear, since the B and K values vary [according to Eq. (2)]. This model can be considered quasi-linear (Kearney and Hunter, 1990), with the EMGσ values specifying the model operating point (e.g., background torque level). The parameters (B_e, B_f, K_e, K_f) were then held constant and the second set of eight trials used to estimate *B[m]* and *K[m]* for the 20 s middle segment. These sequences were each averaged and the resulting (scalar) B and K estimates compared to the "true" parameters estimated strictly from the fixed-mechanical method. Both single-channel unwhitened and four-channel whitened EMG performance were compared.

Next, processed EMG signals were used to estimate "ramp-EMG" viscosity and stiffness parameters as a function of time from the ramp-torque trials. Only four-channel, whitened EMGσ estimates were evaluated. The quasi-linear model of Eq. (3) was again used, with one ramp trial used for training. The parameters (B_e, B_f, K_e, K_f) were then held constant and the second ramp trial used to estimate *B[m]* and *K[m]* as a function of time. These *B[m]* and *K[m]* values were compared to the fixed-mechanical true parameters at the specific MVC locations of the truth data set (10%, 20%, 30%, and 40% MVC extension and flexion).

Finally, some researchers would benefit from single-trial direct estimation of impedance parameters over a range of effort levels without the use of EMG. We utilized our ramp-torque trials to investigate doing so. Modeling a quasi-linear relationship between the background torque trend, $\bar{T}[m]$, and viscosity/stiffness (Hunter and Kearney, 1982; Kearney and Hunter, 1990) was incorporated into Eq. (1) by setting:

$$B[m] = c_B\,\bar{T}[m] \quad \text{and} \quad K[m] = c_K\,\bar{T}[m] \quad (4)$$

giving the model:

$$\Delta T[m] = I_o\ddot{\theta}[m] + \{c_B\bar{T}[m]\}\dot{\theta}[m] + \{c_K\bar{T}[m]\}\Delta\theta[m] \quad (5)$$

where c_B and c_K are fit parameters. Again, a quasi-linear model results in which $\bar{T}[m]$ denotes the operating point. The background torque trend $\bar{T}[m]$ was estimated by subtracting $\Delta T[m]$ from the measured torque. One ramp trial was used for training, then c_B and c_K were held constant and the second ramp trial used to estimate *B[m]* and *K[m]* as a function of $\bar{T}[m]$. These *B[m]* and *K[m]* "ramp-mechanical" parameter values were again compared to the fixed-mechanical true parameters at the MVC locations selected in the truth data set.

For comparisons across subjects, viscosity and stiffness values were normalized to each subject's fixed-mechanical parameter values at 40% extension. Stiffness and viscosity parameter differences were compared statistically in SPSS 24 using repeated measures analysis of variance (RANOVA), assessing all possible interactions. When ε was < 0.75, degrees of freedom was adjusted by the method of Greenhouse-Geisser; and when $0.75 \le \varepsilon < 1$, it was adjusted by the method of Huynh-Feldt, where ε indicates the degree of sphericity ($\varepsilon = 1$ indicates exact sphericity) (Girden, 1992). *Post hoc* pair-wise comparisons were limited to comparing a truth parameter (i.e., estimated strictly from the fixed-mechanical measures during a fixed nominal torque) to results from another method, using paired t-tests with Bonferroni correction for multiple comparisons. A significance level of $p = 0.05$ was used.

3. Results

The mean ± std. dev. baseline inertia (I_o), viscosity (B_o) and stiffness (K_o), respectively, at 0% MVC (arm resting in the

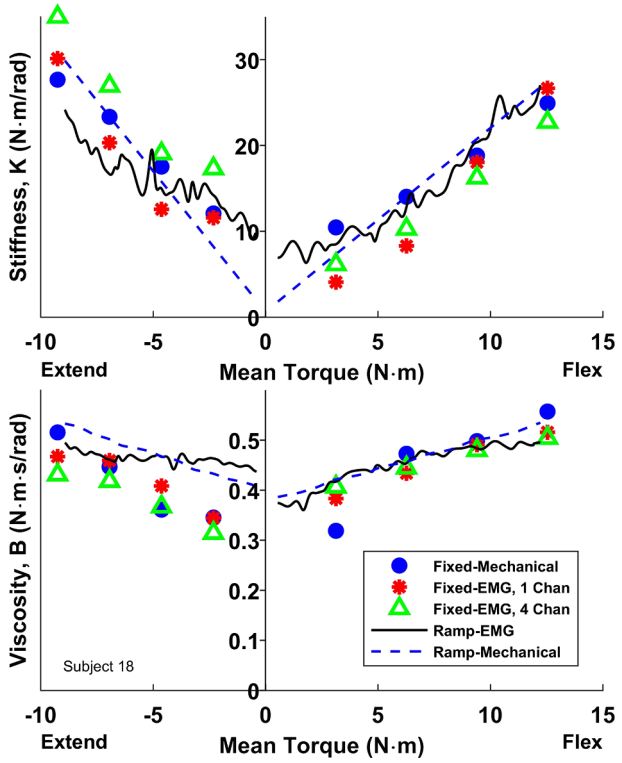

Fig. 4. Viscosity and stiffness estimates for one of the seven subjects.

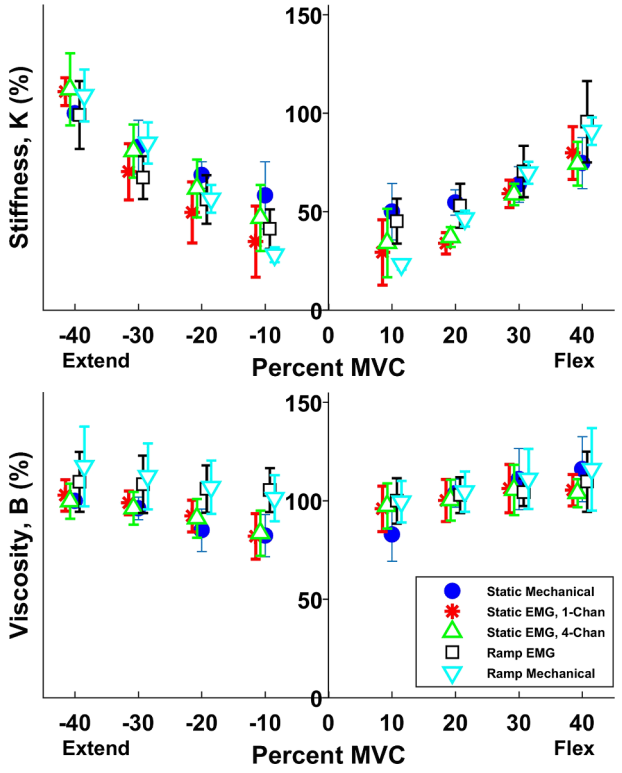

Fig. 5. Mean ± standard deviation viscosity and stiffness estimates (N = 7 subjects), normalized to each subject's fixed-mechanical value at 40% extension. For visibility, results from the five analysis methods (see legend) at each nominal effort level (10, 20, 30, 40% MVC extension/flexion) are slightly offset from each other along the *x*-axis.

manipulandum), were: (61.0 ± 2.68) 10^{-3} N m s^2 rad^{-1}, (2.90 ± 0.100) 10^{-4} N m s rad^{-1} and (5.99 ± 0.318) 10^{-5} N m rad^{-1}. For each ramp contraction, viscosity and stiffness estimates were available continuously throughout the contraction and thus were compared to the eight constant-torque contraction level estimates (Fig. 4). Test trial normalized viscosity and stiffness summary results (mean ± std. dev.) are presented and statistically compared at only these eight constant-torque contraction levels (Fig. 5).

Four two-way RANOVAs were conducted, comprised of separate stiffness and viscosity comparisons for each of extension and flexion efforts (factors: five analysis methods, four effort levels), but each yielded an interaction between analysis method and effort [$F(12, 72) > 5.6$, $p \leq 0.01$]. Since prior studies have already established that both stiffness and viscosity increase with the background effort level (Kearney and Hunter, 1990; Zhang and Rymer, 1997), and because the primary interest of this study was comparison of the standard fixed-mechanical ("true") measures of impedance to the remaining analysis methods, we next computed separate one-way RANOVAs with the effort level fixed [$F(4, 24)$ for each]. Nine of the 16 parameter-effort combinations exhibited no significant differences (Table 1). For the remaining combinations, a limited number of paired differences were found.

4. Discussion

This work set out to evaluate less cumbersome and time-consuming ways in which to estimate total joint impedance, using the fixed-mechanical method as the "truth" standard. Comparing stiffness between the fixed-mechanical method and the other methods (Table 1 and Fig. 5) indicates a primary trend for *lower* stiffness values when estimating with the fixed-EMG model (using either 1-channel unwhitened processing or 4-channel whitened processing)—but only when the background torque was at the lower flexion effort levels (10% and 20% MVC). At these contraction levels, the average stiffness estimates differed by 12–20%. Such differences might be related to the nonlinearity in the relationship between EMG and torque during constant-effort contractions (Solomonow et al., 1986). This issue might be improved by utilizing nonlinear EMG-impedance models in Eqs. (2) and (4). In support of this option, Zhang and Rymer (1997) found a generally linear relationship between stiffness and background muscle torque as torque increased from zero; but this relationship became non-linear in some subjects at the higher background muscle torques. Specifically, background torque increases at the higher torque levels led to less than linear increases in stiffness. Alternatively, the lower fixed-EMG stiffness values might be attributed to the fact that EMGσ does not fall to zero at 0% MVC (due to noise at the electrode-skin interface and electronics noise) (Clancy et al., 2002), thus altering the EMG-impedance relationship in this range. This noise might be mitigated by utilizing more advanced EMG processing [e.g., adaptive Wiener filtering (Clancy and Farry, 2000) and/or power-domain noise subtraction (Clancy, 1991; Hansson et al., 1997; Ortengren, 1996) of EMG "baseline" noise]. Comparing viscosity between the fixed-mechanical ("true") method and the other methods (Table 1 and Fig. 5) indicates a primary trend for *higher* values when estimating from ramp contractions (using either EMG or the mechanical method)—but only when that background torque was at the lowest flexion or extension effort levels (10% MVC). At these levels, the average viscosity estimates differed by 16–22%. Overall, the trend for viscosity and stiffness was to rise with contraction effort. Further, if viscosity results (Fig. 5) are extrapolated using a value of zero at 0% MVC (required, since the viscosity influence of the resting arm and manipulandum was removed from this analysis), then viscosity increases in a less than linear manner (e.g., square root shape) with background torque level. These trends, as well as the absolute values of these parameters, are consistent with the literature (Kearney and Hunter, 1990; Perreault et al., 2004; Zhang and Rymer, 1997). Overall, therefore, the fixed-EMG- and ramp-based measures were reasonable

Table 1
Statistical comparisons at each effort level. Results list statistically significant differences in the *post hoc* *t*-tests (only conducted if the one-way RANOVA was significant) between the fixed-mechanical ("true") method and the listed analysis method. Parentheses give *p*-values.

	Extension Effort Level (MVC)				Flexion Effort Level (MVC)			
	40%	30%	20%	10%	10%	20%	30%	40%
Stiffness: Difference compared to fixed-mechanical ("true")?	–	–	Fixed- EMG 1-Chan Unwhite ($p = 0.03$)	–	Fixed- EMG 1-Chan Unwhite ($p < 0.01$) Fixed-EMG 4-Chan White ($p < 0.01$)	Fixed- EMG 1-Chan Unwhite ($p < 0.01$) Fixed-EMG 4-Chan White ($p < 0.01$)	–	Ramp-Mechanical ($p = 0.02$)
Viscosity: Difference compared to fixed-mechanical ("true")?	–	–	Ramp-EMG ($p < 0.05$)	Ramp-EMG ($p = 0.01$) Ramp-Mechanical ($p = 0.03$)	Ramp-EMG ($p = 0.04$) Ramp-Mechanical ($p = 0.04$)	–	–	–

proxies for the fixed-mechanical ("true") measurements.

Our use of regularization in the model fitting was only found to be critical when the subject was *not* active. To demonstrate, we also computed inertia, viscosity and stiffness values, respectively, for the manipulandum alone as: $(48.1 \pm 0.416)\,10^{-3}\,\mathrm{N\,m\,s^2\,rad^{-1}}$, $(2.30 \pm 0.000)\,10^{-4}\,\mathrm{N\,m\,s\,rad^{-1}}$ and $(4.51 \pm 0.069)\,10^{-5}\,\mathrm{N\,m\,rad^{-1}}$. But, if regression modeling was used *without* regularization, then these and the 0% MVC viscosity values increased by a factor of approximately 10^3, stiffness values increased by a factor of approximately 10^4, and inertia was unaffected. At these low impedance values, stiffness and viscosity values were quite sensitive to the use of regularization. Our tolerance value for rejecting singular values (< 0.005) was rather modest and is well justified in the closely-related EMG-force problem (Clancy et al., 2012), in which the "true" (output force) is measured much more reliably. We next compared regularized vs. unregularized parameters values during the active trials of a subset of two subjects—stiffness values varied by less than 8% and viscosity values by less than 3%. These observations are consistent with regularization theory (Press et al., 1994). When stiffness and viscosity values are near zero, their parameters are not distinguishable in Eq. (1), as each associated term contributes nearly zero torque in the equation. Nearly all of the torque is due to inertia. Regularization purposely choses a fit solution that minimized the stiffness and viscosity fit parameter magnitudes, while inertia is unaffected. During active contractions in which stiffness and viscosity contributions are substantive, these parameter contributions are substantial and, thus, only weakly influenced by regularization.

Although we did not explicitly test for performance differences directly between single-channel unwhitened EMG processing and four-channel whitened EMG processing, no prominent distinctions are evident (Table 1). This result is expected as the advanced (whitened, multi-channel) EMG processors do not change the *average* value of EMGσ, rather they only reduce its *variance* (Clancy and Farry, 2000; Clancy and Hogan, 1994, 1995). Hence, they would not be expected to experience much difference when their average value is compared across a full trial or when only compared across six subject values. But, they would be expected to lower variance in real-time applications in which impedance (and torque) is estimated from EMG.

Our work was limited by avoiding dynamics in the background torque, so would need to be further developed to be applicable to situations in which the operating point changed rapidly—especially since there is evidence of lower stiffness when the background torque (or position) changes dynamically. Nonetheless, our ramp contraction consisted of one half cycle of a ramp occurring over a time span of 50 s. This contraction profile exhibits a fundamental frequency of $1/(100\,\mathrm{s}) = 0.01$ Hz. Experimental work in the literature that found differences in impedance when comparing "static" background contraction conditions to "dynamic" background contraction conditions has done so at much higher fundamental frequencies (those more commonly associated with natural movement). Bennett et al. (1992) found that stiffness dropped (compared to static conditions) during sinusoidal arm movements at 1.6 and 2.1 rad/s (=0.25 and 0.33 Hz). Rouse et al. (2014) studied lower limb impedance during gait, with subjects walking at rates of 85–90 steps/minute (thus, a frequency > 1 Hz). They found lower stiffness during locomotion, by a factor of approximately one half, compared to predicted stiffness during isometric contraction. Ludvig et al. (2017) found lower knee impedance (compared to static conditions) when the leg oscillated ± 0.15 rad (8.6°) at a typical rate of 0.5 Hz. MacNeil et al. (1992) also mention this phenomenon in their study of ankle impedance. They observed lower stiffness during the transient portion of rapid step changes in ankle force. Our own study used changes in background torque that were a factor of 100 lower in frequency, and thus our models treated these changes as quasi-static.

In addition, our work was limited by use of a small sample size (seven subjects), since small sample sizes are biased towards non-significant findings. In particular, to obtain a statistical power of 0.80 in one-way ANOVA with five groups, using a Type I error (α) of 0.05, requires an effect size of approximately 0.55 (Cohen, 1992; Vanbrabant et al., 2015). Thus, only large differences were detectable in this study. Additionally, our testing data were identical in character to our training data—a common (and useful) paradigm in system identification. A resulting limitation is that our reported EMG-impedance errors are representative of this ramp contraction profile, but errors are likely to rise if different contraction profiles are evaluated (i.e., if the model is extrapolated to conditions that differ from those found in the training data).

In our experiments, we applied a torque perturbation and measured the resulting variation in elbow angle. When doing so, it is necessary to account for the dynamics of the manipulandum, since the measured elbow angle is due to the impedance of both the manipulandum and the elbow. We did so by modeling the dynamics of the manipulandum and resting arm during our 0% MVC "calibration" contraction. Thereafter, we subtracted these contributions out of each active trial—those utilizing a constant background torque as well as those utilizing a slow ramp variation in background torque—using the model formed during 0% MVC calibration. This method accounts for manipulandum dynamics in a *serial* fashion within the signal analysis. Alternatively, a number of authors account for manipulandum dynamics via signal analysis methods that *simultaneously* solve for the impedance of the arm/leg and also the manipulandum (de Vlugt et al., 2003; Ludvig et al., 2017; Zhao et al., 2008). Pros for our serial method are that the modeling is simpler and that, to the extent that the manipulandum dynamics are fixed and well modeled from the 0% MVC calibration contraction, system identification of less complex systems is typically more robust as the number of fit parameters is reduced (Ljung, 1999). Pros for the simultaneous technique are that it can more easily adapt to changes in manipulandum dynamics when they are not fixed and that no separate 0% MVC calibration contractions are required.

A limitation of our torque perturbations was that at zero background torque, subjects must generate stiffness in order to stabilize the location of the manipulandum (i.e., to prevent the elbow angle from drifting to one of its extremes, since angle is not constrained by the perturbation). Thus, the arm is unable to fully relax. If, however, angle perturbations had been utilized instead (Kearney and Hunter, 1990), no

such instability results. The arm might more readily relax at the zero background torque condition.

Two common EMG-based measures of muscle co-activation use normalized EMGσ from agonist and antagonist muscles and either compute a co-contraction *index* (CI) based on the area of their overlap (generally normalized by the time duration of overlap) or a co-contraction *ratio* (CR) from agonist and antagonist muscle EMGσ as (Ford et al., 2008; Rosa et al., 2014): $CR = \frac{EMG\sigma_{Agonist}}{EMG\sigma_{Antagonist}}$. While these measures are simple to compute, they have shortcomings. Each measure expresses relative co-activation, not absolute. Thus, a large CI is indicative of a large time duration of overlap, a large area within the overlap, or anything in between. Similarly, a large CR can indicate very large agonist activity, very small antagonist activity, or anything in between. Additionally, the CR is quite unstable when the denominator term (antagonist muscle activity) is near zero. These EMG-based measures also lack physical dimensions (each measure is dimensionless). Hence, they have no direct relation to robust mechanical measures. In contrast, joint mechanical impedance is a well-established mechanical measure, with physical units. Thus, EMG-based estimates of impedance can be used to modulate impedance in physical systems. For example, EMG-based measures of impedance have been used to modulate joint impedance in a laboratory-demonstrated elbow prosthesis (Abul-Haj and Hogan, 1987, 1990). Yet, if desired, impedance can be normalized to provide a relative co-activation measure. (We did so herein, normalizing to the stiffness/viscosity value at 40% extension MVC.)

Historically, direct measures of human mechanical joint impedance have been time-consuming to complete, generally requiring numerous individual perturbations, distributed across a range of fixed operating points (i.e., background torque levels). While estimates based on biomechanical muscle models are emerging (Pfeifer et al., 2012; Sartori et al., 2015), calibration-based system identification methods remain dominant. Further, physical joint impedance is a nonlinear quantity that is a function of the joint range of motion, perturbation frequencies, etc.; resulting in distinct definitions such as quasi-stiffness and short range stiffness (Rack and Westbury, 1974; Rouse et al., 2013; Sartori et al., 2015). Perturbation-based system identification techniques would provide an estimate of quasi-stiffness if the perturbation bandwidth were more limited. More generally, perturbation-based techniques estimate the type of stiffness elicited by the perturbations (Rouse et al., 2013; Sartori et al., 2015) and, thus, can be tailored to match the problem under study.

5. Conclusion

In this work, we demonstrated estimates of total impedance that were statistically similar to traditional perturbation-based measures of fixed background contractions using EMG from a single contraction trial in which the background torque was slowly ramped over a range of effort levels. Once the EMG-impedance model is fit via least squares, impedance can be *estimated* from the surface EMG without the need for perturbations. In addition, our work demonstrated that a single ramp contraction can be used to mechanically *measure* impedance over a range of operating points, even if subsequent EMG-impedance modeling is not desired. These methods are less cumbersome and time-consuming than the existing fixed-mechanical method and less complex than advanced techniques that separate intrinsic vs. reflex stiffness.

Conflict of interest

None declared.

Acknowledgements

Funded in part by the National Institute for Occupational Safety and Health via grant R03 OH007829.

Appendix A. Supplementary material

Supplementary data to this article can be found online at https://doi.org/10.1016/j.jelekin.2019.02.001.

References

Abul-Haj, C., Hogan, N., 1987. An emulator system for developing improved elbow-prosthesis designs. IEEE Trans. Biomed. Eng. 34, 724–737.
Abul-Haj, C.J., Hogan, N., 1990. Functional assessment of control systems for cybernetic elbow prosthesis—Part I: description of the technique. IEEE Trans. Biomed. Eng. 37, 1025–1036.
An, K.N., Cooney, W.P., Chao, E.Y., Askew, L.J., Daube, J.R., 1983. Determination of forces in extensor pollicis longus and flexor pollicis longus of the thumb. J. Appl. Physiol. 54, 714–719.
Andison, C., 2011. EMG-Based Assessment of Active Muscle Stiffness and Co-Contraction in Muscles with Primary and Secondary Actions at the Wrist During Piano Playing. Carleton University, Ottawa, Ontario, Canada.
Bennett, D.J., Hollerbach, J.M., Xu, Y., Hunter, I.W., 1992. Time-varying stiffness of human elbow joint during cyclic voluntary movement. Exp. Brain Res. 88, 433–442.
Burdet, E., Osu, R., Franklin, D.W., Milner, T.E., Kawato, M., 2001. The central nervous system stabilizes unstable dynamics by learning optimal impedance. Nature 414, 446–449.
Cannon, S.C., Zahalak, G.I., 1982. The mechanical behavior of active human skeletal muscle in small oscillations. J. Biomech. 15, 111–121.
Cavallo, G., van de Ruit, M., Schouten, A.C., van Wingerden, J.W., Lataire, J., 2018. Nonparametric identification of time-varying human joint admittance. IFAC PapersOnLine 51–15, 533–538.
Clancy, E.A., 1991. Stochastic Modeling of the Relationship Between the Surface Electromygram and Muscle Torque. Ph.D Thesis. Massachusetts Institute of Technology, pp. 456–469.
Clancy, E.A., Bida, O., Rancourt, D., 2006. Influence of advanced electromyogram (EMG) amplitude processors on EMG-to-torque estimation during constant-posture, force-varying contractions. J. Biomech. 39, 2690–2698.
Clancy, E.A., Farry, K.A., 2000. Adaptive whitening of the electromyogram to improve amplitude estimation. IEEE Trans. Biomed. Eng. 47, 709–719.
Clancy, E.A., Hogan, N., 1994. Single site electromyograph amplitude estimation. IEEE Trans. Biomed. Eng. 41, 159–167.
Clancy, E.A., Hogan, N., 1995. Multiple site electromyograph amplitude estimation. IEEE Trans. Biomed. Eng. 42, 203–211.
Clancy, E.A., Hogan, N., 1997. Relating agonist-antagonist electromyograms to joint torque during isometric, quasi-isotonic, non-fatiguing contractions. IEEE Trans. Biomed. Eng. 44, 1024–1028.
Clancy, E.A., Liu, L., Liu, P., Moyer, D.V., 2012. Identification of constant-posture EMG-torque relationship about the elbow using nonlinear dynamic models. IEEE Trans. Biomed. Eng. 59, 205–212.
Clancy, E.A., Morin, E.L., Merletti, R., 2002. Sampling, noise-reduction and amplitude estimation issues in surface electromyography. J. Electromyo. Kinesiol. 12, 1–16.
Cohen, J., 1992. A power primer. Psychol. Bull. 112, 155–159.
de Vlugt, E., Schouten, A.C., van der Helm, F.C.T., 2003. Closed-loop multivariable system identification for the characterization of the dynamic arm compliance using continuous force disturbances: a model study. J. Neurosci. Meth. 122, 123–140.
Disselhorst-Klug, C., Schmitz-Rode, T., Rau, G., 2009. Surface electromyography and muscle force: limits in sEMG-force relationship and new approaches for applications. Clin. Biomech. 24, 225–235.
Doheny, E.P., Lowery, M.M., FitzPatrick, D.P., O'Malley, M.J., 2008. Effect of elbow joint angle on force-EMG relationships in human elbow flexor and extensor muscles. J. Electromyogr. Kinesiol. 18, 760–770.
Doorenbosch, C.A.M., Harlaar, J., 2003. A clinically applicable EMG-force model to quantify active stabilization of the knee after a lesion of the anterior cruciate ligament. Clin. Biomech. 18, 142–149.
Ford, K.R., van den Bogert, J., Myer, G.D., Shapiro, R., Hewett, T.E., 2008. The effects of age and skill level on knee musculature co-contraction during functional activities: a systematic review. Br. J. Sports Med. 42, 561–566.
Giakas, G., Baltzopoulos, V., 1997. Optimal digital filtering requires a different cut-off frequency strategy for the determination of the higher derivatives. J. Biomech. 30, 851–855.
Girden ER, 1992. ANOVA: Repeated Measures. Sage Publications, pp. 21.
Golkar, M.A., Tehrani, E.S., Kearney, R.E., 2017. Linear parametric varying identification of dynamic joint stiffness during time-varying voluntary contractions. Front. Comput. Neurosci. 11, 35.
Gomi, H., Osu, R., 1998. Task-dependent viscoelasticity of human multijoint arm and its spatial characteristics for interaction with environments. J. Neurosci. 18, 8965–8978.
Gottlieb, G.L., Agarwal, G.C., 1971. Dynamic relationship between isometric muscle tension and the electromyogram in man. J. Appl. Physiol. 30, 345–351.
Guarin, D.L., Kearney, R.E., 2018. Unbiased estimation of human joint intrinsic mechanical properties during movement. IEEE Trans. Neural Sys. Rehabil. Eng. 26, 1975–1984.
Hagg, G.M., Melin, B., Kadefors, R., 2004. Applications in ergonomics. In: Merletti, R., Parker, P.A. (Eds.), Electromyography: Physiology, Engineering, and Noninvasive Applications. IEEE Press/Wiley-Interscience, pp. 343–363.
Hansson, G.A., Asterland, P., Skerfving, S., 1997. Acquisition and analyses of whole-day electromyographic field recordings. In: Hermens, H.J., Hagg, G., Freriks, B. (Eds.), Proceedings of the Second General SENIAM (Surface EMG for Non Invasive

Assessment of Muscles) Workshop, Stockholm, Sweden. Enschede. Roessing Research and Development, The Netherlands, pp. 19–27.
Hashemi, J., Morin, E., Mousavi, P., Hashtrudi-Zaad, K., 2013. Surface EMG force modeling with joint angle based calibration. J. Electromyogr. Kinesiol. 23, 416–424.
Hashemi, J., Morin, E., Mousavi, P., Hashtrudi-Zaad, K., 2015. Enhanced dynamic EMG-force estimation through calibration and PCI modeling. IEEE Trans. Neural Sys. Rehabil. Eng. 23, 41–50.
Hashemi, J., Morin, E., Mousavi, P., Mountjoy, K., Hashtrudi-Zaad, K., 2012. EMG-force modeling using parallel cascade identification. J. Electromyogr. Kinesiol. 22, 469–477.
Hogan, N., Mann, R.W., 1980. Myoelectric signal processing: optimal estimation applied to electromyography—Part II: experimental demonstration of optimal myoprocessor performance. IEEE Trans. Biomed. Eng. 27, 396–410.
Hunter, I.W., Kearney, R.E., 1982. Dynamics of human ankle stiffness: variation with mean ankle torque. J. Biomech. 15, 747–752.
Kawase, T., Kambara, H., Koike, Y., 2012. A power assist device based on joint equilibrium point estimation from EMG signals. J. Robot Mechatron. 24, 205–218.
Kearney, R.E., Hunter, I.W., 1990. System identification of human joint dynamics. CRC Crit. Reviews Biomed. Eng. 18, 55–87.
Kearney, R.E., Stein, R.B., Parameswaran, L., 1997. Indentification of intrinsic and reflex contributions to human ankle stiffness dynamics. IEEE Trans. Biomed. Eng. 44, 493–504.
Liu, P., Liu, L., Clancy, E.A., 2015. Influence of joint angle on EMG-torque model during constant-posture, torque-varying contractions. IEEE Trans. Neural Sys. Rehabil. Eng. 23, 1039–1046.
Ljung, L., 1999. System Identification: Theory for the User. Upper Saddle River. Prentice-Hall, NJ 1–8, 408–452, 491–519.
Ludvig, D., Perreault, E.J., 2012. System identification of physiological systems using short data segments. IEEE Trans. Biomed. Eng. 59, 3541–3549.
Ludvig, D., Plocharski, M., Plocharski, P., Perreault, E.J., 2017. Mechanisms contributing to reduced knee stiffness during movement. Exp. Brain Res. 235, 2959–2970.
MacNeil, J.B., Kearney, R.E., Hunter, I.W., 1992. Identification of time-varying biological systems from ensemble data. IEEE Trans. Biomed. Eng. 39, 1213–1225.
McIntyre, J., Mussa-Ivaldi, F.A., Bizzi, E., 1996. The control of stable postures in the multijoint arm. Exp. Brain Res. 110, 248–264.
Ortengren, R., 1996. Noise and artefacts. In: Kumar, S., Mital, A. (Eds.), Electromyography in Ergonomics. Taylor & Francis, London, pp. 97–107.
Osu, R., Gomi, H., 1999. Multijoint muscle regulation mechanisms examined by measured human arm stiffness and EMG signals. J. Neurophysiol. 81, 1458–1468.
Parker, P., Englehart, K., Hudgins, B., 2006. Myoelectric signal processing for control of powered limb prostheses. J. Electromyo. Kinesiol. 16, 541–548.
Perreault, E.J., Kirsch, R.F., Crago, P.E., 2004. Multijoint dynamics and postural stability of the human arm. Exp. Brain Res. 157, 507–517.
Pfeifer, S., Vallery, H., Hardegger, M., Riener, R., Perreault, E.J., 2012. Model-based estimation of knee stiffness. IEEE Trans. Biomed. Eng. 59, 2604–2612.
Potvin, J.R., Brown, S.H.M., 2004. Less is more: High pass filtering, to remove up to 99% of the surface EMG signal power, improves EMG-based biceps brachii muscle force estimates. J. Electromyo. Kinesiol. 14, 389–399.
Prakash, P., Salini, C.A., Tranquilli, J.A., Brown, D.R., Clancy, E.A., 2005. Adaptive whitening in electromyogram amplitude estimation for epoch-based applications. IEEE Trans. Biomed. Eng. 52, 331–334.
Press, W.H., Flannery, B.P., Teukolsky, S.A., Vetterling, W.T., 1994. Numerical Recipies in C, 2nd ed. Cambridge Univ. Press, New York, pp. 671–681.
Rack, P.M.H., Westbury, D.R., 1974. The short range stiffness of active mammalian muscle and its effect on mechanical properties. J. Physiol. 240, 331–350.
Rancourt, D., Hogan, N., 2001a. Dynamics of pushing. J. Motor Behavior 33, 351–362.
Rancourt, D., Hogan, N., 2001b. Stability in force-production tasks. J. Motor Behavior 33, 193–204.
Rosa, M.C.N., Marques, A., Demain, S., Metcalf, C.D., Rodrigues, J., 2014. Methodologies to assess muscle co-contraction during gait in people with neurological impairment—A systematic literature review. J. Electromyo. Kinesiol. 24, 179–191.
Rouse, E.J., Gregg, R.D., Hargrove, L.J., Sensinger, J.W., 2013. The difference between stiffness and quasi-stiffness in the context of biomechanical modeling. IEEE Trans. Biomed. Eng. 60, 562–568.
Rouse, E.J., Hargrove, L.J., Perreault, E.J., Kuiken, T.A., 2014. Estimation of human ankle impedance during the stance phase of walking. IEEE Trans. Neural Sys. Rehabil. Eng. 22, 870–878.
Sartori, M., Maculan, M., Pizzolato, C., Reggiani, M., Farina, D., 2015. Modeling and simulating the neuromuscular mechanisms regulating ankle and knee joint stiffness during human locomotion. J. Neurophysiol. 114, 2509–2527.
Shin, D., Kim, J., Koike, Y., 2009. A myokinetic arm model for estimating joint torque and stiffness from EMG signals during maintained posture. J. Neurophysiol. 101, 387–401.
Solomonow, M., Guzzi, A., Baratta, R., Shoji, H., D'Ambrosia, R., 1986. EMG-force model of the elbows antagonistic muscle pair. Am. J. Phys. Med. 65, 223–244.
Staudenmann, D., Roeleveld, K., Stegeman, D.F., van Dieen, J.H., 2010. Methodological aspects of EMG recordings for force estimation—A tutorial and review. J. Electromyogr. Kinesiol. 20, 375–387.
Tee, K.P., Franklin, D.W., Kawato, M., Milner, T.E., Burdet, E., 2010. Concurrent adaptation of force and impedance in the redundant muscle system. Biol. Cybern. 102, 31–44.
Thelen, D.G., Schultz, A.B., Fassois, S.D., Ashton-Miller, J.A., 1994. Identification of dynamic myoelectric signal-to-force models during isometric lumber muscle contractions. J. Biomech. 27, 907–919.
Vanbrabant, L., Van De Schoot, R., Rosseel, Y., 2015. Constrained statistical inference: Sample-size tables for ANOVA and regression. Front. Psychol. 5, 1565.
Vredenbregt, J., Rau, G., 1973. Surface electromyography in relation to force, muscle length and endurance. New Develop. Electromyogr. Clin. Neurophysiol. 1, 607–622.
Winter, D.A., 2005. Biomechanics and Motor Control of Human Movement, 3rd ed. John Wiley & Sons Inc, pp. 40–58.
Zhang, L.-Q., Rymer, W.Z., 1997. Simultaneous and nonlinear identification of mechanical and reflex properties of human elbow joint muscles. IEEE Trans. Biomed. Eng. 44, 1192–1209.
Zhao, Y., Ludvig, D., Kearney, R.E., 2008. Closed-loop system identification of ankle dynamics using a subspace method with reference input as instrumental variable. Am Control Conf 619–624.

Chenyun Dai received the B.S. degree from Nanjing University of Aeronautics and Astronautics, Nanjing, China, and the S.M. and Ph.D. degrees from Worcester Polytechnic Institute (WPI), Worcester, MA, all in Electrical Engineering. He has worked as a postdoctoral fellow in the department of Biomedical Engineering at University of North Carolina at Chapel Hill. He is working as an associate professor in the department of Electrical Engineering at Fudan University, China since Feb. 2019. His research interests include biomedical signal processing, system identification and human rehabilitation.

Stephane Martel completed both M. Sc. A. and B.S. degrees in Mechanical Engineering at Sherbrooke University, after which he joined BRP Inc. as a design engineer. He then moved to Juarez in Mexico to supervise BRP product manufacturing. His interests are in system design and modelling.

François Martel is currently completing a Ph.D. degree in Mechanical Engineering at Sherbrooke University, after graduating in Mechanical Engineering from the same institution with both an M. Sc. A. and B.S. degrees. His various R&D internships and international collaborations reinforced his skills in design, mechatronics and identification of physical systems. His research interests are primarily focused on human performance enhancement and safety or system design, in particular advanced support surfaces.

Denis Rancourt received his Ph.D. from MIT in the department of Mechanical Engineering in 1995, after completing a Master's degree in Mechanical Engineering at École Polytechnique de Montréal in 1989. After ten years as a professor in Mechanical Engineering at Laval University, he was appointed Professor in the division of Bioengineering at Sherbrooke University, QC, Canada, in 2003. His expertise in design, modelling and control of physical systems has led him to conduct several contractual R&D projects with various industries and the community, notably, Alpine and Athletics Canada, for the development of new sports equipment for the Vancouver 2010 and London 2012 Paralympics Games. His research interests are primarily focused on human performance enhancement and the prevention of musculo-skeletal injuries through advanced modelling and design work. He is currently leading the Center for Radical Innovation Research at Sherbrooke University and the Research Group Perseus in human performance and safety.

Edward (Ted) A. Clancy received the B.S. degree from Worcester Polytechnic Institute (WPI), and the S.M. and Ph.D. degrees from Massachusetts Institute of Technology (MIT), all in Electrical Engineering. He has worked in industry for medical instrumentation and analysis companies interested in EMG, EEG, ECG and blood pressure, and the defense industry (aircraft instruments and radar). He is Professor of Electrical and Computer Engineering, and of Biomedical Engineering at WPI. He is interested in signal processing, stochastic estimation, applied system identification, and instrumentation; particularly as applied to problems in medical engineering and human rehabilitation.

Supplementary Material

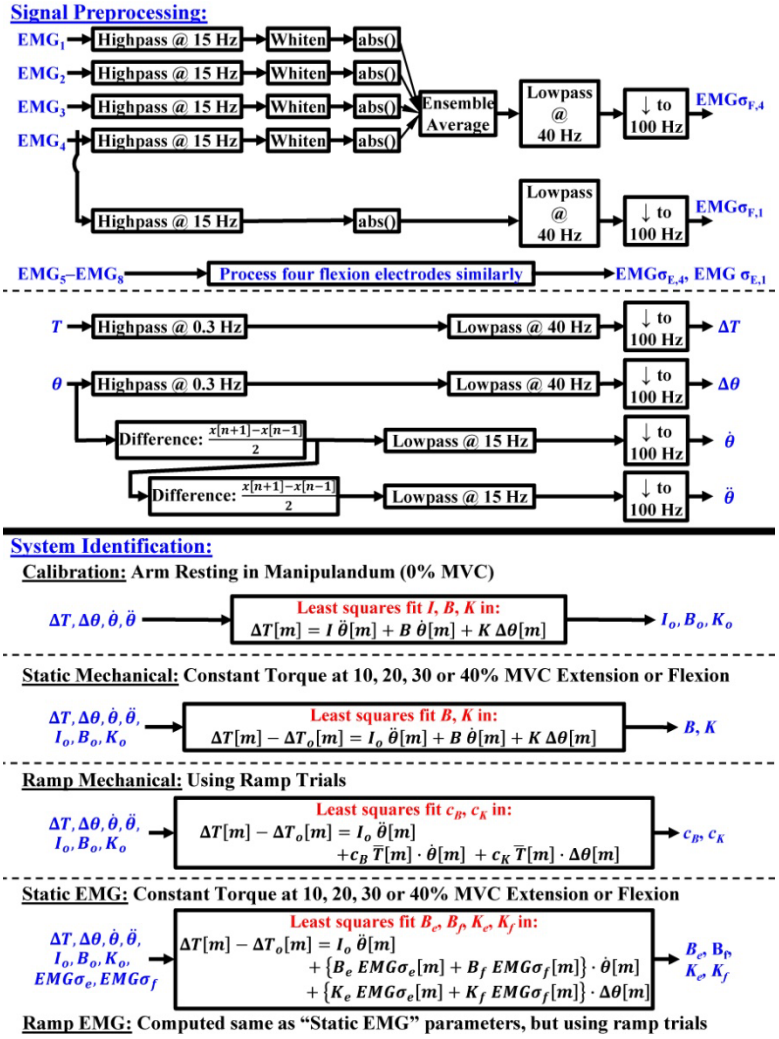

Fig. S1. Graphical summary of signal analysis steps. Unless noted otherwise, all symbols defined in the text. Top depicts preprocessing of the measured signals, where: EMG_1–EMG_4 are from flexion electrodes; EMG_5–EMG_8 are from extension electrodes; EMGσ subscripts E and F denote extension and flexion, respectively; EMGσ subscripts 1 and 4 denote single-channel unwhitened and four-channel whitened, respectively; and n is the sample index at the original sampling rate. Bottom depicts system identification. Calibration is performed once, after which I_o, B_o, and K_o are used to estimate $\Delta T_o[m]$ in subsequent system identification.